Am J Physiol Renal Physiol 299: F167–F177, 2010.
First published May 12, 2010; doi:10.1152/ajprenal.00162.2010.

Regulation of the creatine transporter by AMP-activated protein kinase in kidney epithelial cells

Hui Li,[1] Ramon F. Thali,[3] Christy Smolak,[1] Fan Gong,[1] Rodrigo Alzamora,[1] Theo Wallimann,[3] Roland Scholz,[3] Núria M. Pastor-Soler,[1,2] Dietbert Neumann,[3] and Kenneth R. Hallows[1,2]

[1]*Renal-Electrolyte Division, Department of Medicine and* [2]*Department of Cell Biology and Physiology, University of Pittsburgh School of Medicine, Pittsburgh, Pennsylvania; and* [3]*Department of Biology, Institute of Cell Biology, ETH Zurich, Zurich, Switzerland*

Submitted 18 March 2010; accepted in final form 6 May 2010

Li H, Thali RF, Smolak C, Gong F, Alzamora R, Wallimann T, Scholz R, Pastor-Soler NM, Neumann D, Hallows KR. Regulation of the creatine transporter by AMP-activated protein kinase in kidney epithelial cells. *Am J Physiol Renal Physiol* 299: F167–F177, 2010. First published May 12, 2010; doi:10.1152/ajprenal.00162.2010.— The metabolic sensor AMP-activated protein kinase (AMPK) regulates several transport proteins, potentially coupling transport activity to cellular stress and energy levels. The creatine transporter (CRT; *SLC6A8*) mediates creatine uptake into several cell types, including kidney epithelial cells, where it has been proposed that CRT is important for reclamation of filtered creatine, a process critical for total body creatine homeostasis. Creatine and phosphocreatine provide an intracellular, high-energy phosphate-buffering system essential for maintaining ATP supply in tissues with high energy demands. To test our hypothesis that CRT is regulated by AMPK in the kidney, we examined CRT and AMPK distribution in the kidney and the regulation of CRT by AMPK in cells. By immunofluorescence staining, we detected CRT at the apical pole in a polarized mouse S3 proximal tubule cell line and in native rat kidney proximal tubules, a distribution overlapping with AMPK. Two-electrode voltage-clamp (TEV) measurements of Na^+-dependent creatine uptake into CRT-expressing *Xenopus laevis* oocytes demonstrated that AMPK inhibited CRT via a reduction in its Michaelis-Menten V_{max} parameter. [^{14}C]creatine uptake and apical surface biotinylation measurements in polarized S3 cells demonstrated parallel reductions in creatine influx and CRT apical membrane expression after AMPK activation with the AMP-mimetic compound 5-aminoimidazole-4-carboxamide-1-β-D-ribofuranoside. In oocyte TEV experiments, rapamycin and the AMPK activator 5-aminoimidazole-4-carboxamide-1-β-D-ribofuranosyl 5′-monophosphate (ZMP) inhibited CRT currents, but there was no additive inhibition of CRT by ZMP, suggesting that AMPK may inhibit CRT indirectly via the mammalian target of rapamycin pathway. We conclude that AMPK inhibits apical membrane CRT expression in kidney proximal tubule cells, which could be important in reducing cellular energy expenditure and unnecessary creatine reabsorption under conditions of local and whole body metabolic stress.

proximal tubule; metabolism; *Xenopus* oocytes; target of rapamycin; *SLC6A8*

AMP-ACTIVATED PROTEIN KINASE (AMPK) is a ubiquitous metabolic-sensing kinase that exists as an α,β,γ heterotrimer and is activated by cellular energy depletion (elevated ratios of intracellular AMP to ATP concentration) and other cellular stresses (e.g., Ca^{2+} stress). AMPK activation involves phosphorylation of the catalytic α-subunit at Thr^{172} ($pThr^{172}$) by upstream AMPK kinases that include the LKB1 complex and the Ca^{2+}/calmodulin-dependent kinase kinase-β (24). AMPK regulates a wide variety of cellular processes, including metabolic pathways, cell growth [via tuberous sclerosis complex (TSC2) in the mammalian target of rapamycin (mTOR) pathway], inflammation, protein synthesis, gene transcription, and membrane transport (16, 23, 37). We and others have shown that AMPK regulates a growing number of epithelial ion transport proteins, including the CFTR Cl^- channel, the epithelial Na^+ channel (ENaC), the Na^+-K^+-$2Cl^-$ cotransporter (NKCC2), the KCa3.1 channel, and the vacuolar H^+-ATPase (4, 6, 10, 13, 17, 19–21, 29, 48). AMPK-dependent inhibition of these and other diffusive ion transport pathways may serve to minimize the dissipation of ionic gradients under conditions of cellular energy depletion. Concomitantly, AMPK activation enhances cellular nutrient uptake through increased plasma membrane expression and transcription of glucose and fatty acid transport proteins (16). Thus, recent studies suggest an emerging paradigm whereby AMPK couples membrane transport to cellular metabolism, preserving the intracellular ionic environment, limiting ATP consumption, and defending the ability of cells to generate ATP and, thereby, continue vital processes in the face of metabolic stress. AMPK-dependent regulation of transport proteins may be indirect and mediated through common cellular signaling pathways and trafficking regulators (e.g., the ubiquitin ligase Nedd4-2, which regulates the ENaC) (4). We have thus considered that AMPK may regulate other important membrane transport proteins, the expression or activities of which are modulated by cellular energy status or other cellular stresses.

The creatine transporter (CRT; *SLC6A8*) is a 635-amino acid Na^+-Cl^--coupled electrogenic cotransporter (with a 2 Na^+:1 Cl^-:1 creatine stoichiometry) (9, 12) that mediates creatine uptake into a variety of cells, including neuronal cells, skeletal and cardiac muscle cells, and intestinal and kidney epithelial cells (15, 34). Like AMPK, the creatine kinase (CK)-phosphocreatine (PCr) system is important in the maintenance of ATP homeostasis in tissues that have a high and rapidly fluctuating energy requirement (32, 47). Specifically, PCr, formed by CK-dependent phosphorylation of creatine, serves as an important energy reservoir for ATP production. The CK-PCr system also serves as a mechanism for the transport of high-energy phosphate from intracellular sites of energy production (e.g., glycolysis or mitochondrial respiration) to sites of energy consumption (e.g., membrane pump ATPases) (3, 36, 47). In addition, it appears that CRT expression is required to provide creatine for its conversion to PCr in cells that cannot manufacture creatine, such as brain and muscle cells (8). Its importance in these cells is underscored by naturally occurring

Address for reprint requests and other correspondence: K. R. Hallows, Univ. of Pittsburgh, Renal-Electrolyte Division, S976 Scaife Hall, 3550 Terrace St., Pittsburgh, PA 15261 (e-mail: hallows@pitt.edu).

mutations in *SLC6A8* that can cause developmental delays, mental retardation, severe language problems, skeletoneuromuscular disorders, and cardiomyopathy (42).

In intestinal and renal epithelial cells, CRT expression at the apical membrane appears to have a different main role. In the intestine, CRT mediates alimentary creatine uptake and transepithelial creatine transport (34). In the kidney, it mediates the first step of creatine reclamation in the nephron, a process that is critical for total body creatine homeostasis, thereby limiting the need for de novo creatine synthesis in the liver and other organs (12). De novo creatine synthesis is energetically costly and requires a significant fraction of the total body methyl group donor potential in the form of *S*-adenosylmethionine (41). Under normal conditions, the kidney effectively salvages creatine from the urine, and adult men on a creatine-free diet excrete little creatine. However, significant amounts of creatine are excreted in the urine following toxic exposures to doxorubicin (33) or lithium (27). Similarly, it has long been recognized that urinary creatine excretion is dramatically increased under an inadequate diet, fasting, and other muscle mass-reducing conditions (26, 45), where AMPK activity is expected to be elevated in cells throughout the body (24). Indeed, creatine import for energy storage into cells would be unnecessary under conditions of starvation, when the body is in a catabolic state, and it would be energetically wasteful, as it would tend to dissipate cellular ionic gradients and necessitate greater Na^+-K^+-ATPase activity. Specifically, the CRT uses an inward Na^+ gradient to move creatine into the cell. Although this process does not expend energy directly, the influx of Na^+ enhances the activity of the Na^+-K^+-ATPase on the basolateral membrane of the cell, and this pump consumes ATP in this process.

A detailed understanding of the regulation of CRT is lacking, but it has been recently reported that CRT is stimulated by mTOR (38, 39). Interestingly, AMPK is an upstream inhibitor of mTOR via its activation of tuberin (TSC2) in the tuberous sclerosis complex (37), providing a potential mechanism for AMPK-dependent regulation of CRT. Furthermore, it has been recently demonstrated that significant AMPK activation occurs in rat kidney following induction of ischemia through ligation of the renal artery (31). Given the common signaling pathways, the central role of the creatine-PCr system in cellular energy homeostasis (46), and the previous observation that metabolic depletion inhibits creatine reabsorption by the kidney, we hypothesized that AMPK may inhibit CRT activity at the plasma membrane of cells in the kidney and other tissues.

In this study, we examined the localization of CRT and AMPK in rat kidney tissue and in a mouse S3 proximal tubule cell line. We also measured CRT-dependent transport in the presence or absence of the AMPK activator 5-aminoimidazole-4-carboxamide-1-β-D-ribofuranoside (AICAR) in the *Xenopus* oocyte expression system using two-electrode voltage clamp (TEV) and in polarized S3 cells through [^{14}C]creatine uptake fluxes. We also measured changes in apical membrane expression of CRT in S3 cells by cell surface biotinylation as a function of AMPK activation. Finally, we tested the role of the mTOR pathway in the AMPK-dependent regulation of CRT in oocyte TEV studies. We found that AMPK regulates CRT plasma membrane expression in oocytes and kidney proximal tubule cells, potentially through a mechanism involving the mTOR pathway.

MATERIALS AND METHODS

Reagents and chemicals. All chemical compounds were purchased from Sigma unless otherwise stated. AICAR and 5-aminoimidazole-4-carboxamide-1-β-D-ribofuranosyl 5′-monophosphate (ZMP) were purchased from Toronto Research Chemicals. [^{14}C]creatine was obtained from Moravek Biochemicals. EZ-Link sulfo-NHS-SS-biotin was obtained from Pierce.

Antibodies. Custom-made immunopurified anti-CRT antibodies recognizing the NH_2 terminus of the CRT were obtained by immunization of rabbits with a synthetic peptide comprising amino acids 14–27 of rat *SLC6A8* (GenBank accession no. NM_017348.2, Anawa, Switzerland). In addition, the following antibodies were obtained: anti-hemagglutinin (HA; HA.11, Covance); anti-AMPK-α and anti-pThr^{172} AMPK-α (AMPK-α-pThr^{172}; Cell Signaling); β-actin (Sigma); mouse anti-ZO-1 and Cy3-coupled phalloidin (Invitrogen); horseradish peroxidase-conjugated secondary IgGs (Amersham Biosciences); and biotin-conjugated Cy3-coupled goat anti-mouse and Cy5-coupled goat anti-rabbit antibodies (Jackson Immunologicals).

Kidney tissue preparation and confocal immunofluorescence microscopy. All animals were treated according to approved protocols by the Institutional Animal Care and Use Committee at the University of Pittsburgh. Adult male rats were perfused via the left ventricle with PBS at pH 7.4 at 37°C and then with paraformaldehyde (4%)-lysine-periodate buffer, as described previously (22). The kidneys were harvested, cut in transverse sections, and further fixed overnight at 4°C in paraformaldehyde (4%)-lysine-periodate. After fixation, tissues were washed, quenched in NH_4Cl, and cryoprotected in 30% sucrose in PBS-azide. Tissues were embedded in Tissue-Tek, and 4-μm cryosections were obtained using a Reichert-Frigocut cryostat (22). The sections were rehydrated in PBS and used for immunolabeling experiments employing the anti-CRT antibody following an antigen retrieval technique (5, 22). For colabeling of CRT and AMPK, the tissue was immunolabeled with the anti-CRT antibody (1:4,000 dilution) and then with biotin-conjugated secondary goat anti-rabbit antibody (1:1,000 dilution). For amplification of the CRT antibody signal, we used a tyramide signal amplification (TSA) kit (Perkin Elmer) according to the manufacturer's instructions; then the same tissue sections were immunolabeled with an anti-AMPK-α antibody (1:50 dilution) in DAKO diluent followed by goat anti-rabbit secondary antibody coupled to Cy5 (1:100 dilution). For immunolabeling of CRT alone, anti-CRT antibody (1:100 dilution) was followed by Cy5-coupled goat anti-rabbit antibody (1:100 dilution). Immunolabeled tissues were imaged using a laser confocal microscope (Leica) at identical settings for all samples, and images were imported into Adobe Photoshop, as described elsewhere (22).

Constructs. For generation of cRNA, the pHAC1 CRT-C-NN (wild-type rat CRT HA-tagged at the NH_2 terminus) (43) was subcloned by PCR into the dual mammalian-oocyte expression vector pMO (4) using its *Not*I and *Xba*I restriction sites to generate the pMO-HA-CRT plasmid. The forward primer was 5′-AGT-CAGTCGCGGCCGCACCATGTACCCATACGATGTTCC-3′, and the reverse primer was 5′-TTCCTCTAGATCACATGACACTCTC-CACC-3′. All clones were confirmed by DNA sequencing.

Oocyte TEV measurements. Xenopus laevis oocytes were harvested, treated with collagenase, and maintained as described previously (6). Oocytes were injected with 30 ng of cRNA encoding HA-tagged CRT. Experiments were performed at room temperature 5–6 days after the injection. TEV recordings were performed at a holding potential of −60 mV. The control (superfusate-ND96) solution contained 96 mM NaCl, 2 mM KCl, 1.8 mM $CaCl_2$, 1 mM $MgCl_2$, and 5 mM HEPES, pH 7.4. Creatine was added to the solution at the indicated concentrations. NaOH was used to titrate the final solutions to pH 7.4. TEV recordings were performed 6 h after microinjection of 40 mM potassium-ZMP (K-ZMP, an AMPK activator) or K-gluconate (control) into the oocytes (32 nl/oocyte) at various concentrations of external creatine. Currents were then fitted

by nonlinear least-squares regression to the Michaelis-Menten equation ($V = V_{max}/\{1 + (K_m/[creatine])\}$) using Igor Pro software (Wavemetrics).

Cell culture. Mouse S3 proximal tubule cells, originally derived by dissection of cells from S3 proximal tubule segments from a Brinster transgenic mouse [Tg(SV4OE)Bri7] carrying the large-T antigen of the SV40 virus, as described elsewhere (28), were a kind gift of Dr. Simon Atkinson. Cells were used at *passage 82–90* and cultured in the same medium used to culture the mpkCCD$_{c14}$ cell line (2). This medium is composed of equal volumes of DMEM and Ham's F-12 plus 60 nM sodium selenate, 5 μg/ml transferrin, 2 mM glutamine, 50 nM dexamethasone, 1 nM triiodothyronine, 10 ng/ml epidermal growth factor, 5 μg/ml insulin, 20 mM D-glucose, 2% (vol/vol) FBS, and 20 mM HEPES, pH 7.4 (reagents from Invitrogen and Sigma). Cells were maintained at 37°C in a humidified 5% CO_2-95% air incubator with medium changes every other day and passaged approximately twice weekly. S3 cells were then subcultured onto different-sized Transwell permeable filter supports (0.4-μm pore size; Corning Costar) and grown 5–7 days prior to use in experiments to allow for cell polarization (polarized S3 cells).

Immunofluorescence labeling and confocal microscopy of polarized S3 cells. For immunofluorescence (IF) staining, polarized S3 cells on Transwell filters (0.33-cm^2 surface area) were pretreated with 1 mM AICAR or vehicle at 37°C for 2–3 h prior to fixation in 2% paraformaldehyde in PBS buffer for 30 min and then permeabilized by the addition of 1% PBS + 1% BSA + 0.1% Triton X-100 for 10 min, as described elsewhere (18). After an additional wash with PBS, filters were immunolabeled with primary anti-CRT antibody (1:50 dilution) in DAKO diluent, along with mouse anti-ZO-1 (1:100 dilution), for 75 min and then with secondary goat anti-rabbit antibody conjugated with Cy5 (1:100 dilution) and secondary goat anti-mouse antibody conjugated with Cy3 (1:800 dilution). In additional experiments, cells were labeled with Cy3-coupled phalloidin (1:1,000 dilution) to stain F-actin. Filters were mounted in Poly-Mount (Polysciences) and imaged in a Leica confocal microscope using a ×40 objective with identical laser and stack acquisition and *x-z* reconstruction settings for all samples. Images were imported into Adobe Photoshop for further analysis and presentation.

Transfection and immunoblotting. Mouse S3 proximal tubule cells were cultured as described above. HEK-293 cells were cultured in DMEM (Sigma) supplemented with 10% FBS, 1% (vol/vol) penicillin (10,000 U/ml), 1% (vol/vol) streptomycin (10,000 μg/ml), and 2 mM L-glutamine (Invitrogen). For overexpression of CRT, cells were grown to 60–80% confluency on dishes prior to transfection (Lipofectamine 2000, Invitrogen) with the empty vector pMO (Con) or pMO-HA-CRT. At 24 h after transfection, cells were washed with ice-cold PBS prior to lysis in PBS containing 1% Triton X-100, 2 mM EDTA, 1 mM phenylmethylsulfonyl fluoride, 1 mM DTT, and 1× complete protease inhibitor cocktail (Roche). After incubation on ice for 15 min, lysates were centrifuged at 17,000 *g* for 15 min at 4°C, and the supernatants were supplemented with 4× SDS Laemmli sample buffer. Subsequent to heating at 65°C for 15 min, 30 μg of total lysate were separated by SDS-PAGE on a 4–12% gradient gel (Nu-PAGE, Invitrogen), transferred to a nitrocellulose membrane, and immunoblotted with primary antibody [anti-HA (1:500 dilution) or anti-CRT (1:1,000 dilution)] overnight at 4°C and then with goat anti-mouse or anti-rabbit secondary antibody for 1 h at room temperature.

Surface biotinylation assays. Polarized S3 cells grown on Transwell filters (4.67-cm^2 surface area) were treated with 1 mM AICAR or vehicle for 2 h prior to apical surface biotinylation assays. Cells were washed three times for 5 min with ice-cold PBS containing Mg^{2+} and Ca^{2+} with agitation on ice to remove medium. The apical membrane was biotinylated using 1 mg/ml EZ-Link sulfo-NHS-SS-biotin in PBS for 30 min. The basolateral surface was incubated in PBS. The biotinylation reaction was then quenched by addition of ice-cold 10% FBS-containing medium to the apical surface. Monolayers were washed three times with ice-cold PBS prior to lysis in PBS containing 1% Triton X-100, 2 mM EDTA, 1 mM phenylmethylsulfonyl fluoride, and 1× complete protease inhibitor cocktail (Roche) on ice for 15 min. Protein concentration of the postnuclear supernatant was determined, and 1 mg of protein was combined with streptavidin-Sepharose beads (Pierce) and incubated on a rotator overnight at 4°C. Samples from the streptavidin beads were washed three times in lysis buffer and collected in 2× Laemmli sample buffer containing 10% DTT. The proteins were heated to 65°C for 15 min, separated by SDS-PAGE on a 4–12% gradient gel (Nu-PAGE), and subjected to Western blot analysis using anti-AMPK-α-pThr^{172}, anti-CRT, and anti-β-actin antibodies.

[^{14}C]creatine uptake flux measurements. Polarized S3 cells grown on Transwell filters (1.12-cm^2 surface area) were treated with AICAR (1 mM) for 2 h prior to and during uptake assays, which were performed on the basis of previously described methods (34). Cells were serum-starved for 30 min at 37°C in Hanks' buffer and then washed twice with Krebs-Ringer-HEPES (KRH) buffer [10 mM HEPES (pH 7.4), 4.7 mM KCl, 2.2 mM $CaCl_2$, 1.2 mM $MgSO_4$, 1.2 mM KH_2PO_4, 10 mM glucose, and 120 mM NaCl]. Uptake assays were performed by apical application of KRH buffer (+ AICAR if appropriate) containing 10 μM [^{14}C]creatine (10 mCi/mmol; Moravec Biochemicals) for 45 min at 37°C ($n = 3$ for each condition). The competitive CRT substrate β-guanidinopropionic acid (GPA, 1 mM) was applied in some fluxes so that background non-CRT-mediated uptake, which amounted to ~10% of the total uptake, could be subtracted. For termination of creatine uptake, the uptake medium was aspirated and the cells were washed twice with 0.5 ml of ice-cold KRH buffer in which 120 mM LiCl was substituted for NaCl. S3 cells were solubilized with 80 μl of lysis buffer. First, samples were taken to determine protein concentrations using the Bradford technique (Bio-Rad). Then aliquots from each sample were analyzed by Western blotting to assess AMPK phosphorylation (anti-AMPK-α-pThr^{172}). Fifty microliters of lysate was counted in 3 ml of advanced safety LSC scintillation cocktail (Fisher Scientific) in a liquid scintillation counter. Results were normalized by protein concentration and subtracted by background (GPA-sensitive counts).

Coprecipitation assays. Glutathione *S*-transferase (GST) pull-down assays were performed using methods described previously (6, 21). Briefly, NH_2-terminal HA-tagged CRT (pMO-HA-CRT), AMPK-β_1 (pMT2-HA-AMPK-β_1), and AMPK-γ_1 (pMT2-HA-AMPK-γ1), along with NH_2-terminal GST-tagged AMPK-α_1 (pEBG-AMPK-α_1) or GST alone (pEBG vector), were coexpressed through transient transfection into HEK-293 cells 1 day prior to experimentation. Monolayers were washed with ice-cold PBS prior to lysis in PBS containing 1% Triton X-100, 2 mM EDTA, 1 mM phenylmethylsulfonyl fluoride, and 1× complete protease inhibitor cocktail on ice for 15 min. Protein concentration of the postnuclear supernatant was determined, and 1 mg of protein was combined with glutathione (GSH)-agarose beads (Pierce) and incubated overnight at 4°C. Samples from the GSH-agarose beads were washed three times in lysis buffer and collected in 2× Laemmli sample buffer containing 10% DTT. The proteins were heated to 65°C for 15 min, separated by SDS-PAGE (Nu-PAGE 4–12% gradient gel, Invitrogen), and subjected to Western blot analysis using anti-HA and anti-GST antibodies.

Statistical analysis. Statistical analyses were performed using StatView (SAS) or SigmaPlot (Jandel Scientific) software. ANOVA was used to compare data obtained from different batches of oocytes for TEV experiments. For other biochemical experiments, statistics were performed using unpaired or paired Student's *t*-tests. $P < 0.05$ was considered significant.

RESULTS

CRT and AMPK localize at the apical pole in rat kidney proximal tubules. First, the cellular and subcellular distribution of CRT and AMPK in fixed rat kidney tissue was examined

(Fig. 1). Immunolabeling in kidney for CRT and the catalytic AMPK-α subunit revealed staining for both proteins at or near the brush border membrane of proximal tubules (Fig. 1, *A* and *C*). To demonstrate CRT and AMPK colocalization within the same section, we used a tyramide signal amplification (TSA) approach, because both antibodies were raised in rabbit. When we performed coimmunolabeling of the CRT (Fig. 1*B*) using TSA, followed by immunolabeling of AMPK (Fig. 1*C*), we observed a partially overlapping distribution of CRT and AMPK immunostaining at or near the apical membrane of this epithelium in proximal tubules (Fig. 1*D*). There was a more granular and discontinuous appearance of CRT staining after TSA (Fig. 1*B*) than without amplification (Fig. 1*A*), an artifact that likely limits the degree of apparent colocalization with AMPK using this approach. In tissues immunolabeled with only secondary antibodies (no primary antibodies), there was minimal nonspecific staining under identical acquisition settings (Fig. 1, *E–G*).

AMPK activation inhibits Na^+-dependent creatine uptake via CRT into oocytes through a reduction in V_{max}. To test whether and how AMPK regulates CRT expression, we performed TEV experiments to compare the activity of this electrogenic $2Na^+$-Cl^--creatine cotransporter expressed in *X. laevis* oocytes as a function of AMPK activation. We measured CRT-dependent currents at a holding potential of −60 mV in oocytes expressing rat CRT with various concentrations of creatine in the external buffer. Typical current sweeps obtained with various creatine concentrations 6 h following microinjection of the AMP-mimetic compound K-ZMP vs. K-gluconate are shown in Fig. 2*A*. Microinjection of the AMPK activator K-ZMP inhibited creatine-dependent currents by 30–40% compared with control (K-gluconate-injected) oocytes with 30 and 300 μM creatine in the buffer (Fig. 2*B*). To better discern the functional mechanism for the AMPK-dependent inhibition of the CRT, we measured CRT-mediated currents at various concentrations of extracellular creatine (0, 15, 30, 100, and 300 μM) after injection of K-ZMP or K-gluconate. We then fitted the data through nonlinear least-squares regression to the Michaelis-Menten equation (see MATERIALS AND METHODS) to derive estimates of maximal CRT activity (V_{max}) and the apparent affinity of CRT for creatine (K_m) as a function of AMPK activation (Fig. 2*C*). Currents within each experiment

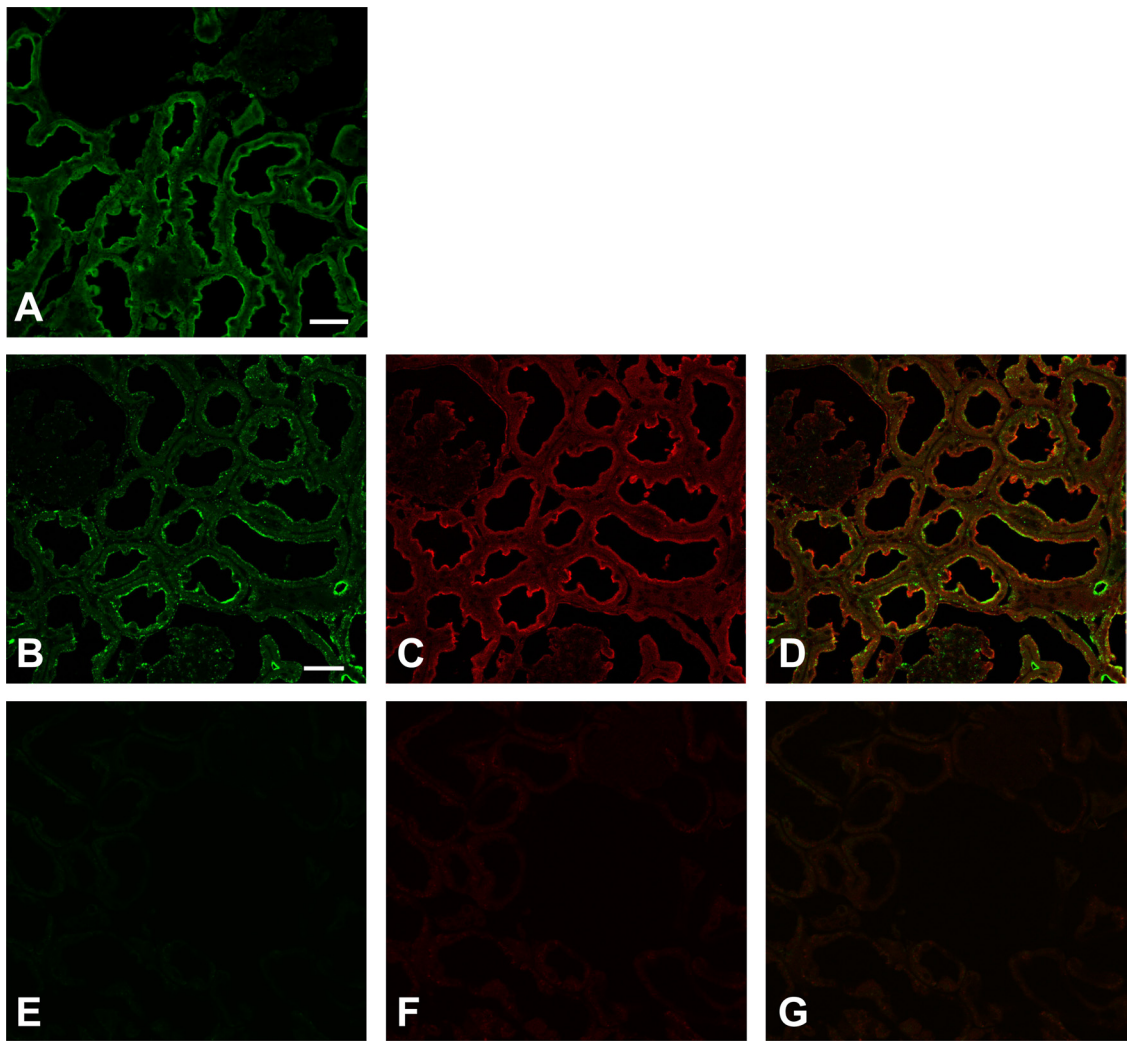

Fig. 1. Creatine transporter (CRT) and AMP-activated protein kinase (AMPK) localize at the apical pole in rat kidney proximal tubules. *A–C*: confocal microscopic images of control rat kidney immunolabeled using an anti-CRT antibody alone (*A*, green) or an anti-CRT antibody amplified by tyramide signal amplification (*B*) and then using an anti-AMPK-α antibody (*C*, red). *D*: regions of colocalization of CRT and AMPK-α at the apical pole of proximal tubule cells (yellow). Scale bars, 100 μm. *E–G*: little nonspecific staining in tissues incubated in the absence of primary antibody.

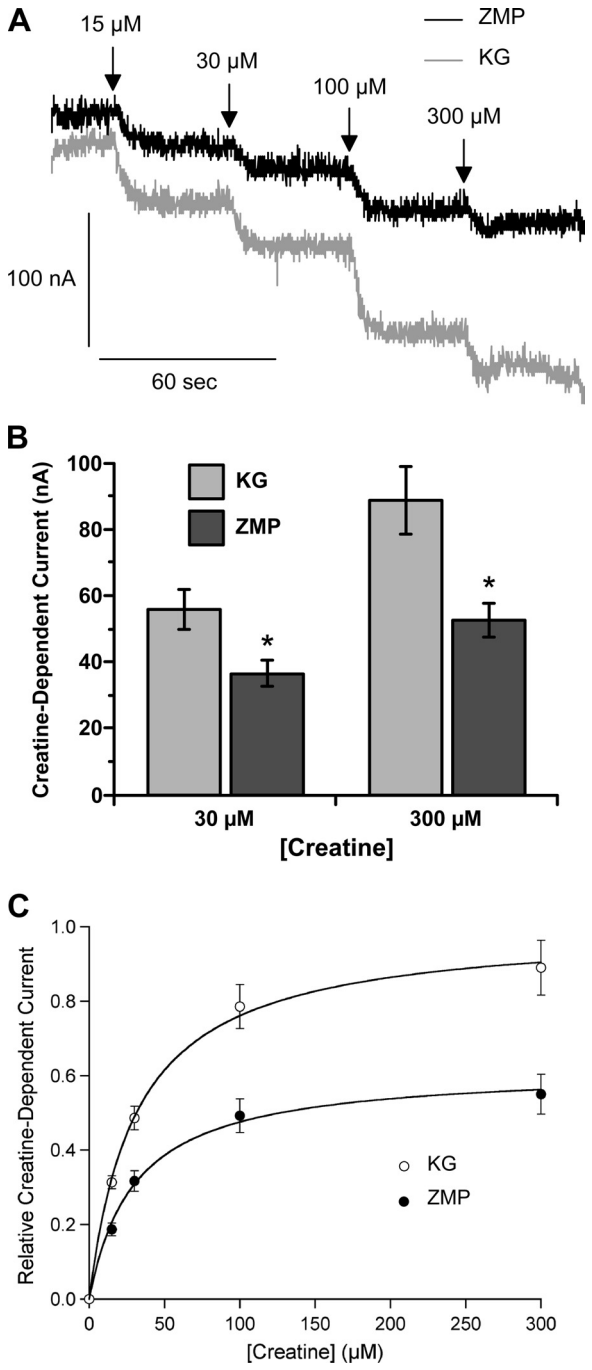

Fig. 2. AMPK activation inhibits CRT-dependent currents in *Xenopus laevis* oocytes. *A*: representative traces of CRT-dependent inward (downward) currents at different concentrations of buffer creatine in the presence of potassium 5-aminoimidazole-4-carboxamide-1-β-D-ribofuranosyl 5′-monophosphate (ZMP) or potassium gluconate (KG). *B*: CRT-dependent currents (means ± SE) were significantly inhibited (30–40%) by the AMPK activator ZMP compared with KG control after 6 h of treatment in the presence of 30 and 300 μM creatine. *$P < 0.05$ relative to KG (2-tailed, unpaired *t*-tests; $n = 24$ oocytes, $N = 3$ batches per condition). *C*: relative CRT-dependent currents measured at various creatine concentrations 6 h after injection of ZMP or KG and then fitted by nonlinear least-squares regression to the Michaelis-Menten equation. V_{max} for each experiment was normalized by the mean V_{max} for KG ($n = 24$ oocytes, $N = 3$ batches per condition). The AMPK activator ZMP caused a 38 ± 2% reduction in V_{max} but had no effect on K_m.

were normalized to the mean calculated V_{max} parameter for K-gluconate-injected oocytes. Injection with the AMPK activator K-ZMP significantly reduced the V_{max} of the CRT by 38 ± 2% compared with that of K-gluconate control-injected oocytes. However, the apparent affinity of CRT for creatine was not affected by the AMPK activator ($K_m = 30.2 \pm 3.5$ μM for K-ZMP treatment vs. 31.3 ± 2.3 μM for K-gluconate treatment). These findings imply that inhibition of CRT activity by AMPK may occur through a reduction in plasma membrane expression of CRT in oocytes.

S3 proximal tubule cells redistribute CRT from the apical pole to the cytoplasm following incubation with the AMPK activator AICAR. To more directly test whether AMPK inhibits CRT activity and apical membrane expression in a more physiologically relevant cell system, we used immortalized cells derived from the S3 segment of the kidney proximal tubule of an SV40 transgenic mouse (28), which were grown on Transwell filters to allow for polarization. We first performed time-course experiments to check for AMPK activation by treatment of S3 cells with 1 mM AICAR (Fig. 3*A*). By immunoblotting for the activated form of AMPK using a phosphospecific antibody (anti-AMPK-α-pThr^{172}), we found that AMPK was well activated by 1 mM AICAR treatment for 2 h in S3 cells, and further activation occurred at later time points (Fig. 3*A*). Because of potential compensatory cellular responses occurring over longer treatment times with the AMPK activator, we focused on the acute effects of AICAR treatment on CRT distribution and activity in these cells at 2–3 h. Immunofluorescence labeling of polarized S3 cells grown on filters with or without AICAR for 2 h prior to fixation and staining is shown in Fig. 3*B*. CRT apical immunolabeling was qualitatively less in cells treated with the AMPK activator (AICAR) than in cells treated with vehicle alone. Specifically, the proportion of total cellular CRT staining apical to (above) the tight junction marker (ZO-1) was substantially greater in vehicle-treated S3 cells than in the AICAR-treated cells (Fig. 3*B*). To account for possible changes in cellular architecture as a function of AICAR treatment, we performed additional staining with phalloidin to delineate the actin cytoskeletal network of polarized S3 cells under both treatment conditions (Fig. 3*C*). AICAR- and vehicle-treated cell monolayers had a similar cytoskeletal actin cellular distribution with a preserved cortical actin web (Fig. 3*C*). Therefore, the decrease in apparent CRT apical pole localization with AICAR treatment appears to be due to a true change in subcellular distribution, rather than a loss of cellular polarity or a disruption of the cortical actin web.

Immunoblotting of CRT-expressing HEK-293 cells. Multiple immunoreactive bands for the CRT on Western blot have been previously described and may vary greatly depending on tissue or cell type (35, 43). To demonstrate the specificity of the CRT antibody used for confocal IF staining and immunoblotting, cell lysates from vector-alone or HA-tagged CRT-transfected HEK-293 cells were analyzed by immunoblotting using anti-HA and anti-CRT antibodies (Fig. 4, *lanes 1–4*). Both antibodies revealed similar signal patterns in CRT-overexpressing HEK-293 cells: very prominent bands at ~120 kDa, more strong bands at 45–50 and 55–60 kDa, and an additional weaker band at 65–75 kDa. These findings suggest that the CRT antibody specifically recognizes CRT. The vector-alone-transfected cells probed with anti-CRT antibody (*lane 1*) dem-

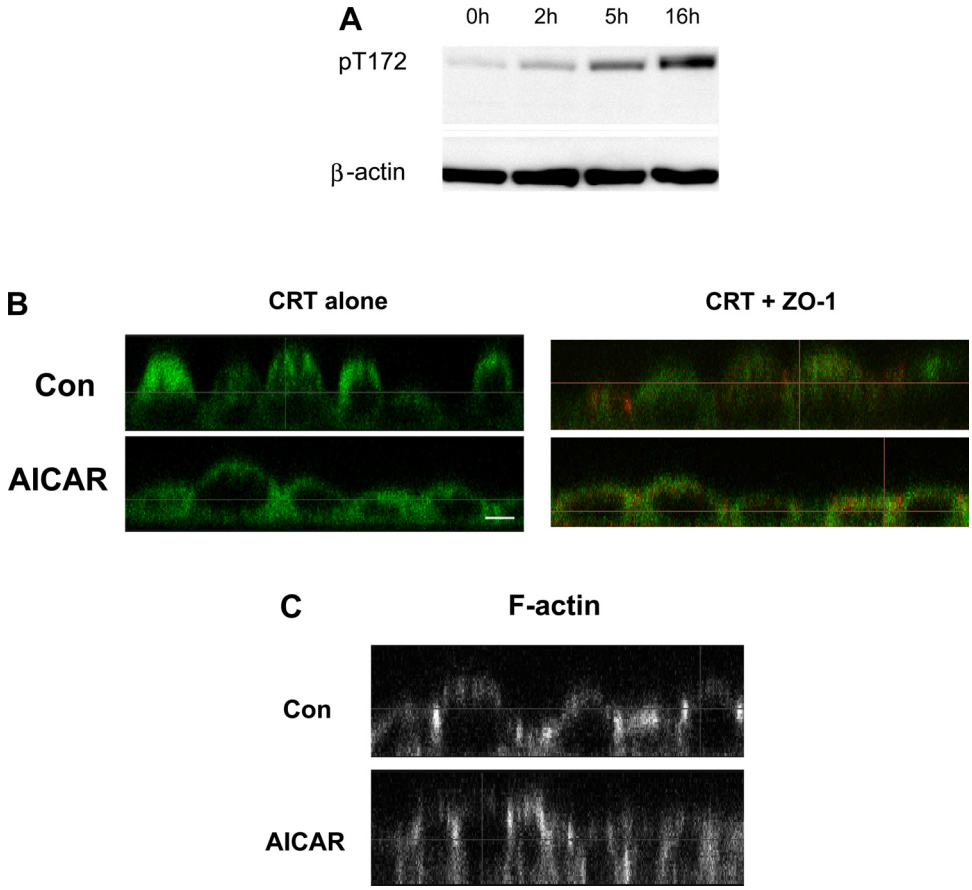

Fig. 3. AMPK activation inhibits apical pole localization of CRT in mouse S3 proximal tubule cells, as determined by immunofluorescence confocal microscopy. *A*: time course of 5-aminoimidazole-4-carboxamide-1-β-D-ribofuranoside (AICAR)-mediated AMPK activation, as measured by immunoblotting of phosphorylated (Thr^{172}) AMPK-α (pT172) in S3 cell lysates. AICAR treatment (1 mM) for 2–16 h induced a significant upregulation of phosphorylated (Thr^{172}) AMPK-α compared with untreated cells at *time 0* under conditions of equivalent protein loading (β-actin control). *B*: AICAR-induced cytoplasmic redistribution of CRT in polarized S3 cells grown on Transwell filters, as shown by *x-z* reconstructions of confocal microscope image stacks of S3 cell monolayers immunolabeled using anti-CRT antibody (green) alone or anti-CRT antibody and an anti-ZO-1 antibody (red) grown under control conditions (Con) or in the presence of 1 mM AICAR for 2 h. *C*: Cy3-coupled phalloidin staining of S3 cell monolayers treated with vehicle (Con) or 1 mM AICAR for 2 h. Images are representative of ≥3 different filter sets and treatments. Scale bar, 10 μm.

onstrated very weak signals corresponding to the lower three bands in the HA-CRT-overexpressing cells, suggesting that there may be low levels of endogenous CRT expression in these cells. To establish the CRT immunoblot signal pattern in S3 proximal tubule cells and test whether cellular host factors may modulate CRT processing, we compared immunoblots of HEK-293 cells and S3 cells transfected with HA-tagged CRT and then immunoblotted using anti-HA antibody (Fig. 4, *lanes 3–6*). The signal pattern observed with expression of HA-CRT in S3 cells differed significantly from that in HEK-293 cells: in S3 cells the uppermost band occurred at 90–95 kDa, and the middle 65- to 75-kDa band was absent (Fig. 4, *lane 6*). These findings indicate that cellular processing of the CRT at the mRNA and/or protein level may differ as a function of host cell type.

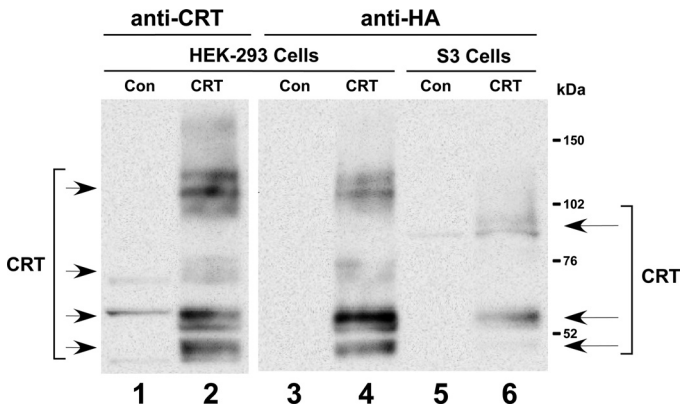

Fig. 4. Complex signal pattern of CRT revealed by immunoblotting. HEK-293 (*lanes 1–4*) or S3 (*lanes 5–6*) cells were transiently transfected with empty vector (Con) or a plasmid encoding the hemagglutinin (HA)-tagged CRT. One-day-posttransfection cell lysates were separated by SDS-PAGE and analyzed by immunoblotting using the anti-CRT (*lanes 1* and *2*) or anti-HA (*lanes 3–6*) antibody. Both antibodies revealed similar immunoblot signal patterns after transfection with HA-CRT in HEK-293 cells, identifying 4 major bands (short arrows on *left*). However, the signal pattern observed in HA-CRT-transfected S3 cells (*lane 6*; long arrows on *right*) differed from that in HA-CRT-transfected HEK-293 cells (*lane 4*), suggesting that cellular processing of the CRT at the mRNA and/or protein level differs as a function of host cell type.

Surface biotinylation and [^{14}C]creatine uptake flux measurements in mouse S3 proximal tubule cells following treatment with the AMPK activator AICAR. To better quantify changes in apical plasma membrane CRT expression following AMPK activation in polarized S3 proximal tubule cells, we performed apical domain-specific surface biotinylation studies to label CRT present in the apical membrane using sulfo-NHS-SS-biotin, which covalently reacts with extracellular Lys residues in proteins. Polarized S3 cells were treated with 1 mM AICAR or vehicle for 2 h prior to apical surface biotin labeling. AICAR treatment enhanced mean AMPK cellular activity to almost four times that of control-treated filters (Fig. 5*A*), while CRT apical plasma membrane expression decreased by 30–40% with AICAR treatment relative to that of control-treated filters (Fig. 5*B*). Interestingly, only the uppermost CRT band at 90–95 kDa appears to be present in the biotinylated apical membrane pool. Together, the results from Figs. 3 and 5 demonstrate that AMPK activation in polarized kidney S3

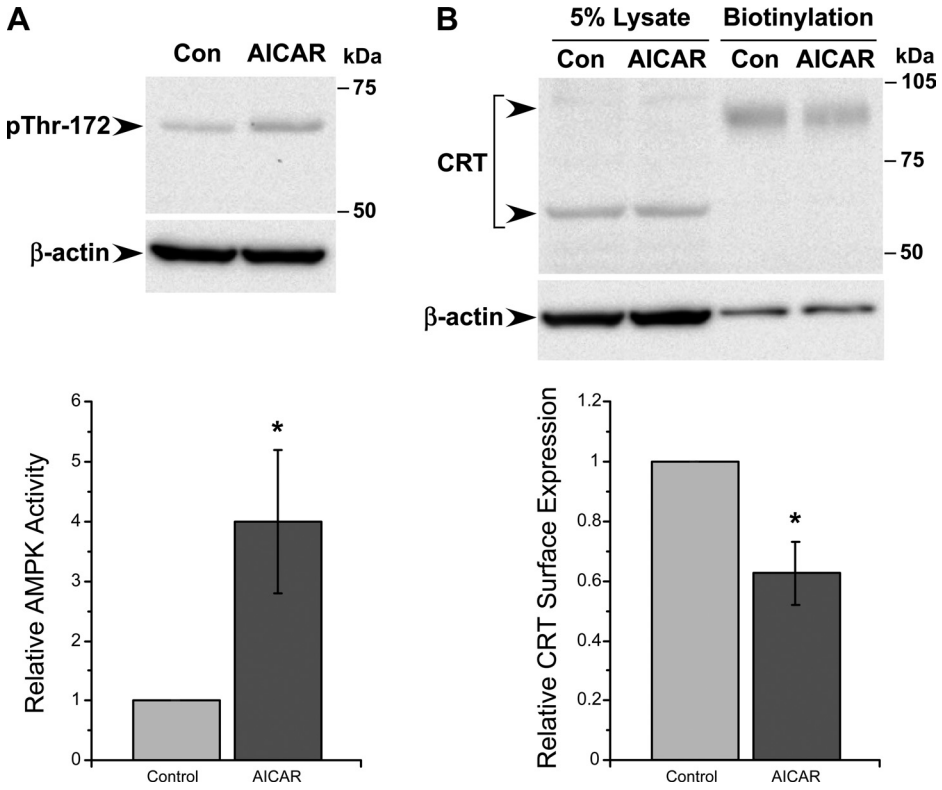

Fig. 5. AMPK activation inhibits apical surface expression of CRT in mouse S3 proximal tubule cells, as measured by biotinylation. *A*: AMPK activity as measured by immunoblotting of phosphorylated (Thr^{172}) AMPK-α (pThr-172) in polarized S3 cell lysates treated with vehicle (Con) or 1 mM AICAR for 2 h under conditions of equal protein loading (β-actin). Quantification (means ± SE) of phosphorylated (Thr^{172}) AMPK-α signal normalized to β-actin signal is shown relative to control (*bottom*). $*P < 0.05$ ($n = 4$ replicate experiments). *B*: immunoblot of CRT in 5% of whole cell lysates or biotinylated protein samples from polarized S3 cell monolayers grown under control conditions (Con) or treated with the AMPK activator AICAR. AICAR-mediated AMPK activation inhibited surface CRT expression (biotinylated CRT) by 30–40% relative to vehicle control, as measured by quantification (means ± SE) of CRT band intensity in the biotinylated fraction divided by that in the cell lysate and expressed relative to that in control cells (*bottom*). $*P < 0.05$ ($n = 4$ experiments). Relatively small amount of β-actin present in the biotinylated fraction (<2% of total cellular β-actin) likely represents binding of the cortical actin cytoskeleton to intrinsic membrane proteins (e.g., Na^+/H^+ exchanger isoform 3) present at the apical membrane of these proximal tubule-derived S3 cells. A variety of apical membrane transport proteins have been shown to interact directly or indirectly with the actin cytoskeleton (30).

proximal tubule cells is associated with an inhibition of apical membrane expression of the CRT, which is consistent with our observation that AMPK activation decreased the V_{max} of exogenously expressed CRT in *Xenopus* oocytes (Fig. 2).

To test whether AMPK inhibits CRT-mediated creatine uptake in polarized S3 proximal tubule cells, [^{14}C]creatine uptake assays from the apical surface were performed under these conditions in the presence or absence of 1 mM AICAR. Uptake assays under both treatment conditions were performed in the presence or absence of 1 mM GPA, a competitive substrate of the CRT, to derive CRT-specific influx rates (34). Additional control experiments confirmed that CRT-specific creatine influx rates were linear during the 45-min uptake flux period used for these measurements (data not shown). In this series of experiments, 1 mM AICAR treatment enhanced mean AMPK cellular activity to almost three times that of control-treated filters (Fig. 6*A*), while CRT-mediated [^{14}C]creatine influx was inhibited by ~20% with AICAR treatment relative to control filters (Fig. 6*B*). Therefore, the loss of apical plasma membrane CRT expression following treatment with the AMPK activator AICAR was associated with a parallel loss of CRT functional transport activity.

AMPK interacts with CRT in cells. To investigate potential mechanisms for the regulation of CRT by AMPK, we first tested whether AMPK interacted with CRT when epitope-tagged versions of these proteins were expressed in HEK-293 cells. GST pull-down assays were performed on lysates from cells that were transfected to express HA-tagged CRT, along

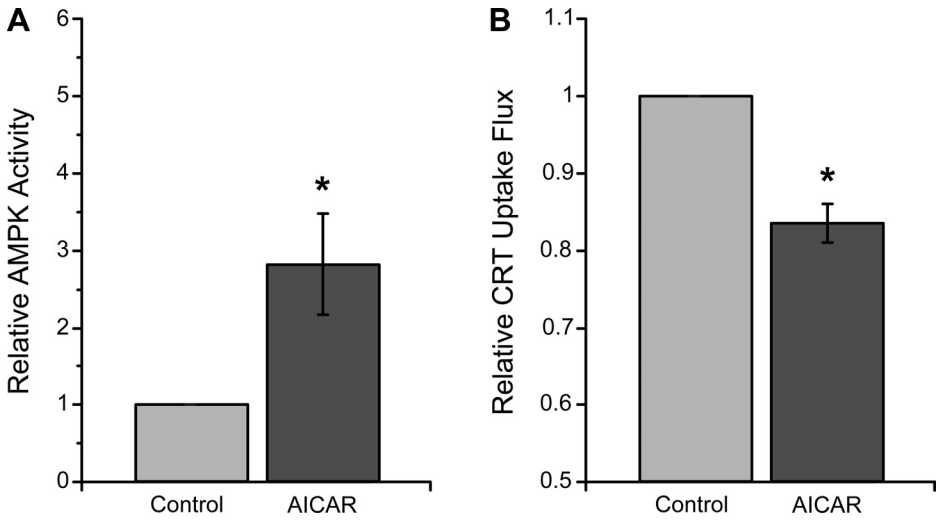

Fig. 6. AMPK activation inhibits CRT-mediated [^{14}C]creatine uptake in mouse S3 proximal tubule cells. Polarized mouse proximal tubule S3 segment cells were grown on Transwell filters. *A*: relative AMPK activity as measured by phosphorylated (Thr^{172}) AMPK-α immunoblotting following treatment with AICAR (1 mM, 2 h) vs. vehicle. Values are means ± SE. $*P < 0.05$ ($n = 3$). *B*: relative CRT uptake assays. Krebs-Ringer-HEPES buffer was applied in the presence or absence of AICAR containing 10 μM [^{14}C]creatine on the apical side for 45 min at 37°C ($n = 3$ per condition). The competitive CRT substrate β-guanidinopropionic acid (1 mM) was added in parallel CRT uptake flux measurements as a control (not shown). Resulting non-CRT-mediated [^{14}C]creatine uptake (generally ~10% of total) was considered background, and this value was subtracted from total uptake values. AICAR induced a ~20% inhibition in CRT-dependent [^{14}C]creatine uptake. $*P < 0.05$ ($n = 3$).

with GST-tagged AMPK-α_1 and HA-tagged AMPK-β_1 and -γ_1 or GST alone (Con, Fig. 7). Samples of cell lysates (Input) or of the proteins affinity-purified from the lysates on GSH-agarose beads (GST pull-down) were immunoblotted using anti-HA (Fig. 7*A*) or anti-GST (Fig. 7*B*) antibodies. As a positive control, the HA-tagged AMPK-β_1 and -γ_1 subunits of the AMPK holoenzyme complex were efficiently pulled down by the GST-AMPK-α_1 bound to GSH-agarose beads, but not by GST alone. Similarly, pull down of HA-tagged CRT by GST-AMPK-α_1 was significant. These results suggest that AMPK-α_1 binds to CRT when expressed in HEK-293 cells, either directly or indirectly. However, additional studies failed to detect any significant in vitro phosphorylation of CRT expressed in and then immunoprecipitated from HEK-293 cell lysates and subsequently exposed to purified AMPK holoenzyme (data not shown). These findings, along with localization studies in kidney tissue (Fig. 1), suggest that although AMPK and CRT may coexist within a regulatory complex in cells, CRT regulation by AMPK may be occurring by a mechanism that does not involve direct phosphorylation of CRT by AMPK.

AMPK may inhibit CRT via an indirect mechanism involving the mTOR pathway. It has been recently reported that CRT is stimulated by mTOR (38), and AMPK is a well-characterized upstream inhibitor of mTOR (37). To investigate whether AMPK may inhibit CRT via an indirect mechanism involving the mTOR pathway, we injected cRNAs to express CRT and mTOR into *Xenopus* oocytes, which were used for TEV measurements of CRT currents 5–6 days after microinjection. An approach described previously to demonstrate regulation of CRT by the mTOR pathway (38) was used to treat oocytes with vehicle (DMSO) or 50 nM rapamycin, an inhibitor of mTOR, 3 days before experimentation. Oocytes were then microinjected with K-ZMP (to activate AMPK) or K-gluconate (control) 5–6 h before TEV measurements, as described above. As observed in oocytes expressing CRT alone (Fig. 2), the AMPK activator ZMP inhibited CRT-dependent currents in oocytes expressing CRT and mTOR together by ~30% (Fig. 8, *left*). Rapamycin pretreatment inhibited CRT-dependent currents relative to vehicle to a similar extent as ZMP (Fig. 8). However, there was no additive inhibitory effect of ZMP microinjection in the rapamycin-pretreated oocytes (Fig. 8, *right*), suggesting that the ZMP-dependent inhibition of CRT may act through the mTOR pathway.

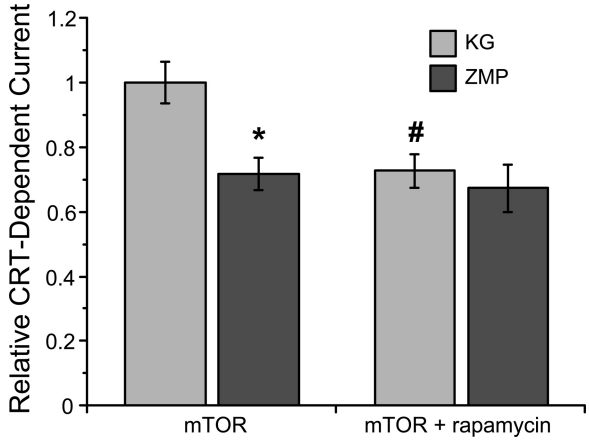

Fig. 8. AMPK regulation of CRT may involve the mammalian target of rapamycin (mTOR) pathway. *Xenopus* oocytes were injected with CRT and mTOR cRNAs 5–6 days before 2-electrode voltage-clamp (TEV) measurements and treated with DMSO (vehicle) or 50 nM rapamycin for 3 days before TEV measurements. Oocytes from control and rapamycin-treated groups were then injected with K-ZMP (ZMP) or K-gluconate (KG) 5–8 h before TEV measurements. CRT-dependent current decreased significantly in mTOR-expressing oocytes treated with ZMP compared with control oocytes treated with KG (*left*). ZMP did not have a significant effect in oocytes expressing mTOR and treated with rapamycin (*right*). $*P < 0.05$ and $\#P < 0.05$ vs. mTOR-alone control (n = 17–21 oocytes per condition, N = 3 batches).

DISCUSSION

The kidney is the principal organ for the first step of endogenous creatine synthesis, where guanidinoacetic acid is synthesized by arginine-glycine aminotransferase, an enzyme highly expressed in this organ. Guanidinoacetic acid synthesized by the kidney is then released into the bloodstream and taken up by the liver, where it is methylated to form creatine. Subsequent release from the liver provides creatine to the various target organs (e.g., skeletal and cardiac muscle, brain and neuronal tissue, testis, and others) (for review see Ref. 49). Besides being involved in the endogenous synthesis of creatine, some kidney epithelial cells, especially those in the proximal tubule that are highly active metabolically due to large transcellular ion fluxes driven by ion-pump ATPases, express high levels of CK (14). Similar to muscle and brain cells, they depend on energy-rich PCr and a high PCr-to-ATP ratio for temporal and spatial energy buffering (47). Thus, efficient

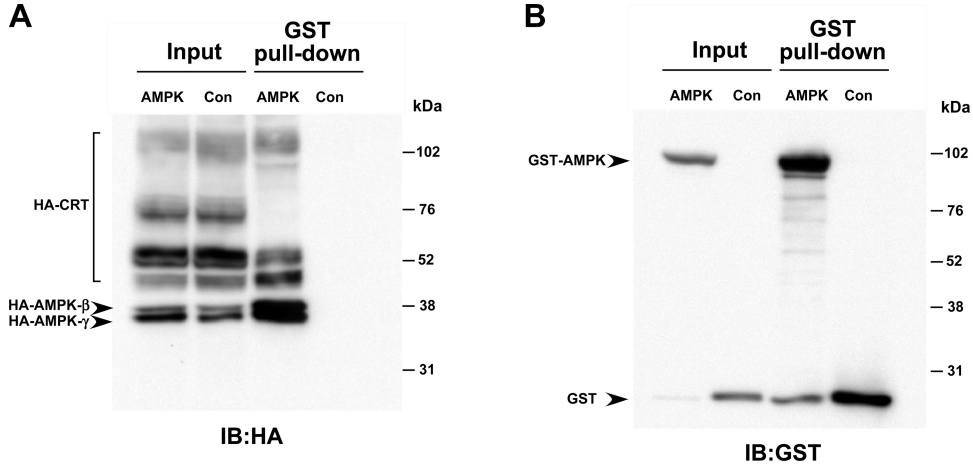

Fig. 7. Glutathione *S*-transferase (GST) pull-down assays detect interaction of CRT with the AMPK-α_1 catalytic subunit. HEK-293 cells were cotransfected with HA-CRT, HA-AMPK-β_1, HA-AMPK-γ_1, and either GST-AMPK-α_1 (AMPK) or GST alone (Con). Cell lysates were used for immunoblot (IB) directly (Input) or for affinity purification using glutathione-agarose beads (GST pull-down). *A*: immunoblot with HA-tagged antibodies to check for interaction of HA-CRT with GST-AMPK-α_1. *B*: Western blot analysis of samples in *A*, with anti-GST antibodies used to verify GST or GST-AMPK-α_1 expression, as well as enrichment by GST pull-down. Images are representative of 3 repeat experiments.

proximal tubular epithelial cell function requires an optimal supply of creatine as a precursor for PCr, which is afforded by expression of the CRT *SCL6A8* at the apical membrane. Indeed, it has been shown that preparations of kidney brush borders and apical membrane vesicles express an apical membrane CRT that is already active in rat fetuses and is developmentally regulated by increase in the density and/or turnover of the transporters (11). However, under conditions of ischemia or metabolic depletion, unabated expression or activity of the CRT at the apical membrane could aggravate cellular metabolic demands by allowing apical Na^+ entry. Ongoing CRT activity would then necessitate greater basolateral Na^+-K^+-ATPase activity and ATP consumption to maintain transcellular ionic gradients. We have thus considered that AMPK, the activity of which is exquisitely sensitive to changes in cellular metabolic status, might be a relevant and important regulator of this transporter.

In this study, we have confirmed that CRT has a prominent apical distribution in kidney proximal tubule and in polarized proximal tubule-derived S3 cells. In rat proximal tubule, immunolabeling for the CRT revealed overlap in some apical regions with the AMPK-α subunit. Moreover, cellular GST pull-down studies showed significant binding of the CRT to AMPK, suggesting that these proteins exist in a complex. This complex could potentially include other proteins, such as the actin cytoskeleton (cf. Fig. 6), which is known to be involved in apical membrane recycling and sorting of a variety of transport proteins (30), and other signaling mediators that are involved in CRT regulation. Our results also suggest that the loss of apical plasma membrane CRT expression following acute treatment with the AMPK activator AICAR was associated with a parallel loss in CRT functional transport activity and that AMPK activation decreased V_{max} and redistributed the transporter from an apical to a more cytosolic distribution in S3 proximal tubule epithelial cells. These findings are consistent with a recent study that demonstrates AMPK-dependent downregulation of the plasma membrane abundance of other Na^+-coupled cotransporters, the glutamate transporters [excitatory amino acid transporters (EAAT3 and EAAT4)] (40). Moreover, consistent with a role for AMPK in the more generalized inhibition of Na^+ reabsorption in the kidney proximal tubule, activation of AMPK in vivo has been recently shown to enhance the tubuloglomerular feedback mechanism and increase the fractional delivery of fluid and Na^+ to the end of the proximal tubule in rats with high dietary NaCl intake (25). AMPK-dependent regulation of transport proteins may be indirect and mediated through common cellular signaling pathways and trafficking regulators. For example, we and others recently showed that ENaC regulation by AMPK is mediated through the ubiquitin ligase Nedd4-2 (1, 4), which regulates a variety of membrane transport proteins (50). When expressed in oocytes, rapamycin and the AMPK activator ZMP inhibited CRT currents, but there was no additive inhibition of CRT by ZMP, suggesting that AMPK may inhibit CRT indirectly via inhibition of the mTOR pathway in cells. The potential pathways downstream of mTOR that are important for AMPK-dependent regulation of CRT are unknown. However, it has been reported that mTOR may act upstream of the serum- and glucocorticoid-regulated kinase isoforms SGK1 and SGK3 in the stimulation of CRT (44). It is also known that CRT is downregulated by activators of protein kinase C (PKC) (9), which is another potential regulatory target of AMPK (7). Further studies to explore the downstream and upstream signaling pathways involved in the AMPK-dependent regulation of CRT in relevant cell model systems and in vivo are warranted.

We envision that the presence of CRT at the apical pole of kidney proximal tubule cells is essential to modulate acutely the metabolic needs of these epithelial cells, in conjunction with AMPK. This study examined acute effects of AMPK activation, which could be relevant under physiological (e.g., with minor fluctuations in cellular energy supply and demand) and pathological (e.g., ischemia) conditions. However, chronic AMPK activation, which may occur on a cellular and a whole body level with chronic starvation or malnutrition, could conceivably have distinct effects on CRT function and may inhibit transepithelial reclamation of creatine in the kidney for the regulation of whole body creatine pools. Under normal conditions, the kidney effectively salvages creatine from the urine, but significant amounts of creatine are excreted in the urine with fasting and other muscle mass-reducing conditions (26, 45), where AMPK activity is expected to be high throughout the body (24). Indeed, creatine uptake into cells as an energy storage buffer could be considered unnecessary under conditions of starvation when the body is in a catabolic state.

A certain fraction of creatine that is reabsorbed from the tubular lumen into kidney epithelial cells is likely to be transported back into the blood, similar to transepithelial creatine transport in gastrointestinal epithelia. Alimentary creatine is taken up from the gut lumen by intestinal epithelial cells and delivered by transepithelial transport into the bloodstream (34). Thus, for creatine reclamation from proximal tubular fluid, it seems likely that a creatine transport system should also exist at the basolateral side of these cells for transepithelial transport of creatine into the bloodstream. However, as observed in intestinal epithelial cells, very little CRT appears to be localized at the basolateral membrane of kidney epithelia cells (Figs. 1 and 3). Therefore, such a transporter is unlikely to be CRT. This assertion is supported by the fact that, if CRT were involved, the combined extracellular Na^+ and Cl^- gradients would move creatine in the opposite direction (i.e., from the blood into the kidney epithelial cell). Thus the nature of this basolateral transporter is still unknown. The function of CRT studied in this setting would therefore primarily represent reabsorption of urinary creatine to preserve whole body creatine metabolism. This notion is supported by the fact that, in models of nephrotoxicity or kidney disease, urinary creatine excretion, which is very low in normal individuals, is highly elevated in doxorubicin- or lithium-induced nephrotoxicity (27, 33).

In summary, this study presents evidence, for the first time, that AMPK regulates CRT in kidney proximal tubule epithelial cells. It appears that AMPK associates with CRT but may not directly phosphorylate the transporter. Further studies are necessary to elucidate the indirect mechanism for AMPK-mediated acute CRT regulation in the kidney.

ACKNOWLEDGMENTS

We thank Dr. Simon Atkinson for mouse S3 cells and Dr. Yu Jiang for the mTOR plasmid. We also thank Christoph Gfeller for dedication to the project.

GRANTS

This study was supported by National Institute of Diabetes and Digestive and Kidney Diseases Grants P30 DK-079307 "Pittsburgh Kidney Research Center," R01-DK-075048 (to K. R. Hallows), and R01-DK-084184 (to N. M. Pastor-Soler), Swiss National Science Foundation Grant 3100A0-114137, and European Union FP6 contract LSHM-CT-2004-005272 (EXGENESIS) and ETHIIRA Graduate Training Fellowships 32/05-3 and 36/05-3.

DISCLOSURES

No conflicts of interest, financial or otherwise, are declared by the authors.

REFERENCES

1. **Almaca J, Kongsuphol P, Hieke B, Ousingsawat J, Viollet B, Schreiber R, Amaral MD, Kunzelmann K.** AMPK controls epithelial Na^+ channels through Nedd4-2 and causes an epithelial phenotype when mutated. *Pflügers Arch* 458: 713–721, 2009.
2. **Bens M, Vallet V, Cluzeaud F, Pascual-Letallec L, Kahn A, Rafestin-Oblin ME, Rossier BC, Vandewalle A.** Corticosteroid-dependent sodium transport in a novel immortalized mouse collecting duct principal cell line. *J Am Soc Nephrol* 10: 923–934, 1999.
3. **Bessman SP, Carpenter CL.** The creatine-creatine phosphate energy shuttle. *Annu Rev Biochem* 54: 831–862, 1985.
4. **Bhalla V, Oyster NM, Fitch AC, Wijngaarden MA, Neumann D, Schlattner U, Pearce D, Hallows KR.** AMP-activated kinase inhibits the epithelial Na channel through functional regulation of the ubiquitin ligase Nedd4-2. *J Biol Chem* 281: 26159–26169, 2006.
5. **Brown D, Lydon J, McLaughlin M, Stuart-Tilley A, Tyszkowski R, Alper S.** Antigen retrieval in cryostat tissue sections and cultured cells by treatment with sodium dodecyl sulfate (SDS). *Histochem Cell Biol* 105: 261–267, 1996.
6. **Carattino MD, Edinger RS, Grieser HJ, Wise R, Neumann D, Schlattner U, Johnson JP, Kleyman TR, Hallows KR.** Epithelial sodium channel inhibition by AMP-activated protein kinase in oocytes and polarized renal epithelial cells. *J Biol Chem* 280: 17608–17616, 2005.
7. **Chen HC, Bandyopadhyay G, Sajan MP, Kanoh Y, Standaert M, Farese RV Jr, Farese RV.** Activation of the ERK pathway and atypical protein kinase C isoforms in exercise- and aminoimidazole-4-carboxamide-1-β-D-riboside (AICAR)-stimulated glucose transport. *J Biol Chem* 277: 23554–23562, 2002.
8. **Chen NH, Reith ME, Quick MW.** Synaptic uptake and beyond: the sodium- and chloride-dependent neurotransmitter transporter family SLC6. *Pflügers Arch* 447: 519–531, 2004.
9. **Dai W, Vinnakota S, Qian X, Kunze DL, Sarkar HK.** Molecular characterization of the human CRT-1 creatine transporter expressed in *Xenopus* oocytes. *Arch Biochem Biophys* 361: 75–84, 1999.
10. **Fraser SA, Gimenez I, Cook N, Jennings I, Katerelos M, Katsis F, Levidiotis V, Kemp BE, Power DA.** Regulation of the renal-specific Na^+-K^+-$2Cl^-$ co-transporter NKCC2 by AMP-activated protein kinase (AMPK). *Biochem J* 405: 85–93, 2007.
11. **Garcia-Delgado M, Garcia-Miranda P, Peral MJ, Calonge ML, Ilundain AA.** Ontogeny up-regulates renal Na^+/Cl^-/creatine transporter in rat. *Biochim Biophys Acta* 1768: 2841–2848, 2007.
12. **Garcia-Delgado M, Peral MJ, Cano M, Calonge ML, Ilundain AA.** Creatine transport in brush-border membrane vesicles isolated from rat kidney cortex. *J Am Soc Nephrol* 12: 1819–1825, 2001.
13. **Gong F, Alzamora R, Smolak C, Li H, Naveed S, Neumann D, Hallows KR, Pastor-Soler NM.** Vacuolar H^+-ATPase apical accumulation in kidney intercalated cells is regulated by PKA and AMP-activated protein kinase. *Am J Physiol Renal Physiol* 298: F1162–F1169, 2010.
14. **Guerrero ML, Beron J, Spindler B, Groscurth P, Wallimann T, Verrey F.** Metabolic support of Na^+ pump in apically permeabilized A6 kidney cell epithelia: role of creatine kinase. *Am J Physiol Cell Physiol* 272: C697–C706, 1997.
15. **Guimbal C, Kilimann MW.** A Na^+-dependent creatine transporter in rabbit brain, muscle, heart, and kidney. cDNA cloning and functional expression. *J Biol Chem* 268: 8418–8421, 1993.
16. **Hallows KR.** Emerging role of AMP-activated protein kinase in coupling membrane transport to cellular metabolism. *Curr Opin Nephrol Hypertens* 14: 464–471, 2005.
17. **Hallows KR, Alzamora R, Li H, Gong F, Smolak C, Neumann D, Pastor-Soler NM.** AMP-activated protein kinase inhibits alkaline pH- and PKA-induced apical vacuolar H^+-ATPase accumulation in epididymal clear cells. *Am J Physiol Cell Physiol* 296: C672–C681, 2009.
18. **Hallows KR, Fitch AC, Richardson CA, Reynolds PR, Clancy JP, Dagher PC, Witters LA, Kolls JK, Pilewski JM.** Up-regulation of AMP-activated kinase by dysfunctional cystic fibrosis transmembrane conductance regulator in cystic fibrosis airway epithelial cells mitigates excessive inflammation. *J Biol Chem* 281: 4231–4241, 2006.
19. **Hallows KR, Kobinger GP, Wilson JM, Witters LA, Foskett JK.** Physiological modulation of CFTR activity by AMP-activated protein kinase in polarized T84 cells. *Am J Physiol Cell Physiol* 284: C1297–C1308, 2003.
20. **Hallows KR, McCane JE, Kemp BE, Witters LA, Foskett JK.** Regulation of channel gating by AMP-activated protein kinase modulates cystic fibrosis transmembrane conductance regulator activity in lung submucosal cells. *J Biol Chem* 278: 998–1004, 2003.
21. **Hallows KR, Raghuram V, Kemp BE, Witters LA, Foskett JK.** Inhibition of cystic fibrosis transmembrane conductance regulator by novel interaction with the metabolic sensor AMP-activated protein kinase. *J Clin Invest* 105: 1711–1721, 2000.
22. **Hallows KR, Wang H, Edinger RS, Butterworth MB, Oyster NM, Li H, Buck J, Levin LR, Johnson JP, Pastor-Soler NM.** Regulation of epithelial Na^+ transport by soluble adenylyl cyclase in kidney collecting duct cells. *J Biol Chem* 284: 5774–5783, 2009.
23. **Hardie DG.** The AMP-activated protein kinase pathway—new players upstream and downstream. *J Cell Sci* 117: 5479–5487, 2004.
24. **Hardie DG, Hawley SA, Scott JW.** AMP-activated protein kinase—development of the energy sensor concept. *J Physiol* 574: 7–15, 2006.
25. **Huang DY, Gao H, Boini KM, Osswald H, Nurnberg B, Lang F.** In vivo stimulation of AMP-activated protein kinase enhanced tubuloglomerular feedback but reduced tubular sodium transport during high dietary NaCl intake. *Pflügers Arch*. In press.
26. **Hunter A.** The physiology of creatine and creatinine. *Physiol Rev* 2: 586–626, 1922.
27. **Hwang GS, Yang JY, Ryu do H, Kwon TH.** Metabolic profiling of kidney and urine in rats with lithium-induced nephrogenic diabetes insipidus by ^{1}H-NMR-based metabonomics. *Am J Physiol Renal Physiol* 298: F461–F470, 2010.
28. **Kaunitz JD, Cummins VP, Mishler D, Nagami GT.** Inhibition of gentamicin uptake into cultured mouse proximal tubule epithelial cells by L-lysine. *J Clin Pharmacol* 33: 63–69, 1993.
29. **Klein H, Garneau L, Trinh NT, Prive A, Dionne F, Goupil E, Thuringer D, Parent L, Brochiero E, Sauve R.** Inhibition of the KCa3.1 channels by AMP-activated protein kinase in human airway epithelial cells. *Am J Physiol Cell Physiol* 296: C285–C295, 2009.
30. **Mazzochi C, Benos DJ, Smith PR.** Interaction of epithelial ion channels with the actin-based cytoskeleton. *Am J Physiol Renal Physiol* 291: F1113–F1122, 2006.
31. **Mount PF, Hill RE, Fraser SA, Levidiotis V, Katsis F, Kemp BE, Power DA.** Acute renal ischemia rapidly activates the energy sensor AMPK but does not increase phosphorylation of eNOS-Ser^{1177}. *Am J Physiol Renal Physiol* 289: F1103–F1115, 2005.
32. **Neumann D, Schlattner U, Wallimann T.** A molecular approach to the concerted action of kinases involved in energy homoeostasis. *Biochem Soc Trans* 31: 169–174, 2003.
33. **Park JC, Hong YS, Kim YJ, Yang JY, Kim EY, Kwack SJ, Ryu do H, Hwang GS, Lee BM.** A metabonomic study on the biochemical effects of doxorubicin in rats using ^{1}H-NMR spectroscopy. *J Toxicol Environ Health A* 72: 374–384, 2009.
34. **Peral MJ, Garcia-Delgado M, Calonge ML, Duran JM, De La Horra MC, Wallimann T, Speer O, Ilundain A.** Human, rat and chicken small intestinal Na^+-Cl^--creatine transporter: functional, molecular characterization and localization. *J Physiol* 545: 133–144, 2002.
35. **Peral MJ, Vazquez-Carretero MD, Ilundain AA.** Na^+/Cl^-/creatine transporter activity and expression in rat brain synaptosomes. *Neuroscience* 165: 53–60, 2010.
36. **Schlattner U, Tokarska-Schlattner M, Wallimann T.** Mitochondrial creatine kinase in human health and disease. *Biochim Biophys Acta* 1762: 164–180, 2006.
37. **Shaw RJ, Bardeesy N, Manning BD, Lopez L, Kosmatka M, DePinho RA, Cantley LC.** The LKB1 tumor suppressor negatively regulates mTOR signaling. *Cancer Cell* 6: 91–99, 2004.
38. **Shojaiefard M, Christie DL, Lang F.** Stimulation of the creatine transporter SLC6A8 by the protein kinase mTOR. *Biochem Biophys Res Commun* 341: 945–949, 2006.

39. **Shojaiefard M, Christie DL, Lang F.** Stimulation of the creatine transporter SLC6A8 by the protein kinases SGK1 and SGK3. *Biochem Biophys Res Commun* 334: 742–746, 2005.
40. **Sopjani M, Alesutan I, Dermaku-Sopjani M, Fraser S, Kemp BE, Foller M, Lang F.** Downregulation of Na^+-coupled glutamate transporter EAAT3 and EAAT4 by AMP-activated protein kinase. *J Neurochem*. In press.
41. **Stead LM, Brosnan JT, Brosnan ME, Vance DE, Jacobs RL.** Is it time to reevaluate methyl balance in humans? *Am J Clin Nutr* 83: 5–10, 2006.
42. **Stockler S, Schutz PW, Salomons GS.** Cerebral creatine deficiency syndromes: clinical aspects, treatment and pathophysiology. *Subcell Biochem* 46: 149–166, 2007.
43. **Straumann N, Wind A, Leuenberger T, Wallimann T.** Effects of N-linked glycosylation on the creatine transporter. *Biochem J* 393: 459–469, 2006.
44. **Strutz-Seebohm N, Shojaiefard M, Christie D, Tavare J, Seebohm G, Lang F.** PIKfyve in the SGK1 mediated regulation of the creatine transporter SLC6A8. *Cell Physiol Biochem* 20: 729–734, 2007.
45. **Walker JB.** Creatine: biosynthesis, regulation, function. *Adv Enzymol Relat Areas Mol Biol* 50: 177–242, 1979.
46. **Wallimann T, Tokarska-Schlattner M, Neumann D, Epand RM, Epand RF, Andres RH, Widmer HR, Hornemann T, Saks V, Agarkova I, Schlattner U.** The phosphocreatine circuit: molecular and cellular physiology of creatine kinases, sensitivity to free radicals, and enhancement by creatine supplementation. In: *Molecular System Bioenergetics*, edited by Saks V. Weinheim, Germany: Wiley-VCH Verlag, 2007, p. 195–264.
47. **Wallimann T, Wyss M, Brdiczka D, Nicolay K, Eppenberger HM.** Intracellular compartmentation, structure and function of creatine kinase isoenzymes in tissues with high and fluctuating energy demands: the "phosphocreatine circuit" for cellular energy homeostasis. *Biochem J* 281: 21–40, 1992.
48. **Woollhead AM, Scott JW, Hardie DG, Baines DL.** Phenformin and 5-aminoimidazole-4-carboxamide-1-β-D-ribofuranoside (AICAR) activation of AMP-activated protein kinase inhibits transepithelial Na^+ transport across H441 lung cells. *J Physiol* 566: 781–792, 2005.
49. **Wyss M, Kaddurah-Daouk R.** Creatine and creatinine metabolism. *Physiol Rev* 80: 1107–1213, 2000.
50. **Yang B, Kumar S.** Nedd4 and Nedd4-2: closely related ubiquitin-protein ligases with distinct physiological functions. *Cell Death Differ* 17: 68–77, 2010.